Received 3 September 2024, accepted 23 September 2024, date of publication 26 September 2024, date of current version 8 October 2024.

Digital Object Identifier 10.1109/ACCESS.2024.3468465

RESEARCH ARTICLE

Gaussian Process Regression for an Accurate and Uncertainty-Aware Winding Insulation Degradation Prediction

MALIHEH HASHEMI[1], MICHAEL STOLZ[1,2], AND DANIEL WATZENIG[2,3], (Senior Member, IEEE)

[1]Institute of Automation and Control, Graz University of Technology, 8010 Graz, Austria
[2]Virtual Vehicle Research GmbH, 8010 Graz, Austria
[3]Institute of Computer Graphics and Vision, Graz University of Technology, 8010 Graz, Austria

Corresponding author: Maliheh Hashemi (maliheh.hashemi@tugraz.at)

This work was supported in part by iRel40 Project, a European co-funded Innovation Project granted by the Electronic Components and Systems for European Leaderships (ECSEL) Joint Undertaking (JU) under Grant 876659; in part by iRel40 Project from the Horizon 2020 Research Program and Participating Countries; and in part by Austrian Research Promotion Agency (Die Österreichische Forschungsförderungsgesellschaft, FFG).

ABSTRACT ccurate prediction of winding insulation degradation path is critical for preventing catastrophic equipment failures and optimizing maintenance schedules in electric motors (EMs). Existing methods, such as those based on monitoring high-frequency electrical parameters, often rely on point estimates and neglecting the inherent uncertainties associated with real-world degradation processes. This paper proposes a novel approach utilizing Gaussian Process Regression (GPR) to address this limitation. Building upon recent advancements in high-frequency electrical parameter monitoring in which identifying inter-turn insulation creep is a key degradation indicator, this work adopts GPR to predict the degradation path. GPR offers a powerful framework for incorporating uncertainty quantification into the prediction process. It not only excels at interpolation within the observed data range but also provides a distribution of possible future degradation values. This probabilistic approach acknowledges the variability present in both real-world measurements and the inherent process variability of insulation degradation. The prediction results from proposed GPR-based approach are compared to a nonlinear Wiener-process-based model as a conventional method, and a state-of-the-art optimization algorithm. The estimation accuracy in the worst case scenario of the proposed method gives an error of 0.7% which is more accurate than 4.2%, and 50% resulted from the Wiener-process-based model and the commercial optimization solver respectively. These results demonstrate a significant improvement in estimation accuracy by effectively handling both data and process-related uncertainties.

INDEX TERMS Degradation estimation, Gaussian process regression, health monitoring, uncertainty quantification, winding insulation reliability.

I. INTRODUCTION

In electrical rotating machines, the significance of winding insulation for maintaining operational performance and safeguarding safety is absolutely essential [1]. This insulation acts as the pivotal protective layer, reducing the risks of electrical leakages and short circuits which can escalate into system-wide failures. The increasing utilization of electric vehicles (EVs) in various industrial applications highlights the vital importance of consistent insulation reliability. Failures in insulation can lead to interruptions in operations, heightened maintenance costs, shortened equipment lifetime, and occasionally, severe system malfunctions. Deterioration of insulation due to thermal, mechanical, and environmental factors always results in ongoing fluctuations in insulation performance [2], [3].

The associate editor coordinating the review of this manuscript and approving it for publication was Yu Liu.

On the other hand when EMs are employed to EVs, having an extended power density is essential to avoid the adoption of mechanical devices such as gearbox or harmonic derives [4]. However, higher power ratings inevitably lead to a greater thermal load on the motor's windings and push the insulation towards its thermal limits [5]. Therefore, an effective thermal management becomes crucial [6]. According to [7], the lifetime of the commonly used insulation materials will be halved if the temperature increases to an additional 10Â°C. This implies that maximizing the life of insulation through an efficient thermal load management not only reduces the requirement for frequent maintenance or replacements but also guarantees the safe and efficient operation of electric machines [8].

Meanwhile, insulation degradation monitoring in EMs, provides a framework for understanding its behavior, predicting its lifetime, and implementing measures to optimize its lifetime [9]. Although the insulation degradation model is affected by multiple factors other than temperature, proposing a temperature-dependent degradation model has been remarkably successful in understanding the principal impacts on insulation deterioration [10].

Insulation systems' testing and monitoring methods can be categorized into offline and online methods.

Current offline testing methods such as those relying on insulation capacitance and resistance measurements [11], despite industry acceptance, disrupt operations and lack continuous monitoring capabilities. On-line monitoring emerges as the preferred solution for uninterrupted operation and enhanced plant safety.

There are two main approaches to obtain a degradation model through online methods: Physical or microscopic life models and Phenomenological, empirical, or macroscopic life models [12]. Physics-based models, while theoretically comprehensive, are often complex and challenging to implement due to the intricate nature of insulation materials and degradation processes. As a result, phenomenological models are more common because of their practicality, and offering simplified representations that effectively capture degradation behavior. Within phenomenological models, distinctions are made between single stress and multi-stress life models. The Arrhenius equation acquired from the physics of failure acceleration model, as a single-stress approach is widely used [13] to drive a lifetime model for an insulation system. This equation as shown in (1), is a basis of thermal aging model

$$K = A \cdot e^{\left(\frac{-E_a}{RT}\right)} \tag{1}$$

where K is the degradation rate. A is a material's dependent constant, T is the hot-spot temperature for insulation and E_a is the activation energy, R is the universal gas constant ($R = 8.314\, J/(mol^{*}K)$), and T is the absolute temperature in Kelvin [14], [15].

As a limitation, the Arrhenius model is inherently static which means it is designed to work with a fixed temperature, not with temperatures that change dynamically over time. Therefore, when it is applied to materials experiencing fluctuating temperatures, it might not provide an accurate representation of the degradation process.

To overcome this, the proposed model in [16] predicts the motor insulation life through dynamic monitoring of the winding temperature and extends the Arrhenius equation to incorporate several winding temperatures instead of one operating temperature.

More importantly, the basic form of Arrhenius model does not capture the interactions between temperature and other factors such as mechanical stresses due to thermal expansion. To incorporate the cumulative effects of multiple stress factors, [17] presents a multi-stress model which estimates the lifetime of the winding insulation based on the thermal and thermo-mechanical effects. As shown in this model, aging due to simultaneously applied constant stresses can be accurately modeled by the product of the aging rate due to the single stresses, with the addition of a proper correction term. However, one major limitation is that it relies on empirical methods to determine the aging rates for individual stresses and then multiplies these rates to estimate the overall aging. In reality, the interactions between stress factors can be highly nonlinear and may not be accurately represented by a multiplicative model.

On the other hand, stochastic methods can take the effects of interactions into account by describing the insulation degradation process through considering randomness or variability and estimate its reliability using probability distributions [18], [19], [20], [21].

Different stochastic models of degradation processes including the random coefficient regression models [22], inverse Gaussian process [23], and Wiener process [24] have been employed to assess the insulation degradation and estimate its remaining useful lifetime (RUL).

However, integrating stochastic modeling techniques into the deterministic models such as Arrhenius based models takes advantage of the strengths of both to develop a more precise, adjustable, and accurate technique for insulation lifetime prediction [25], [26], [27], [28]. While these methods provide valuable insights, they present significant limitations. The Weibull model, despite its flexibility in modeling various failure rates, relies heavily on accurate parameter estimation, which can be sensitive to the quality and quantity of available data. Additionally, extensive datasets are often required to ensure the reliability and robustness of these models.

As stated earlier, a combination of different factors lead to insulation degradation and create a highly complex and nonlinear problem. Therefore, there are challenges and considerations, such as difficulties in parameter estimation and convergence issues when optimization algorithms are adopted in nonlinear models.

While the existing statistical life models provide valuable insights into the insulation degradation process, they often require extensive life data and can be limited in their ability to model complex interactions between multiple stress factors.

This is where GPR offers significant advantages in terms of simplicity and computational efficiency. In particular, GPR has been recently adopted to predict the degradation of proton exchange membrane fuel cell (PEMFC) in [29], and bearing systems in [30].

It is important to note that although there have been some nonlinear accelerated degradation data modeling solutions, the research on the evaluation of the remaining useful lifetime with an optimization algorithm inference to consider nonlinear accelerated degradation data with applications to insulation degradation is still limited [26].

A. MOTIVATION AND CONTRIBUTIONS

Motivated by the aforementioned limitations, this research contributes to the issue of lifetime estimation specifically for winding insulation by combining data obtained from thermal stress tests and GPR. GPR naturally incorporates uncertainty by defining a probability distribution over all possible functions that could model the degradation process. This includes the possibility of capturing effects from other factors even when only single-stress tests are conducted. The key contributions of this study are:

- **Handling non-linearities:** GPR offers a probabilistic framework that can effectively model the unavoidable variations and non-linearities in insulation degradation. This means it accounts for the complex interactions between various stress factors (e.g., thermal, electrical, mechanical) influencing degradation, providing a more comprehensive understanding beyond the isolated effects of thermal stress alone.
- **Uncertainty quantification:** by incorporating uncertainty estimates into predictions, GPR enhances the reliability and robustness of forecasts, supporting informed decision-making in maintenance strategies.
- **Data and Time efficiency:** unlike existing data-driven approaches that often require large datasets for parameter estimation and validation, GPR can achieve accurate predictions with smaller, more targeted datasets. This capability is particularly advantageous in the context of insulation degradation, where comprehensive datasets may be challenging to obtain due to the long-term nature of degradation processes and the variability in environmental conditions.

The GPR model is trained using data collected during the thermal stress tests and allows for the estimation of the insulation degradation under controlled and stressed conditions. Under working conditions, the insulation system will be affected by other aging factors, such as electrical stress. By defining a space of all possible functions and establishing an uncertainty boundary using a suitable kernel, GPR allows us to overcome the limitation of not explicitly testing for these additional factors. This feature sets GPR as a non-parametric regression method apart from other stochastic extrapolation methods. Subsequently, the results are carefully extrapolated to normal operating conditions using appropriate conversion techniques based on the physical processes influenced by temperature. This extrapolation step requires cautious consideration due to potential limitations of the Arrhenius equation at significantly different temperature ranges.

Finally, by analyzing the predicted degradation path under normal conditions, the remaining useful lifetime (RUL) of the insulation is estimated.

The remainder of this article is organized as follows: Section II the background mathematics of GPR are briefly reviewed and then a degradation model using experimental data and GPR is proposed. In section III, a generalized degradation model is obtained from stress level to normal working condition through kernel definition with calculated kernel parameter. Then, the approximated RUL distribution is given in Section IV. To evaluate the performance of the proposed method, discussion and simulation results are provided in Section V. In the end, this article is concluded in Section VI.

II. MODELING OF INSULATION DEGRADATION UNDER THERMAL AGING

A. ACCELERATED DEGRADATION TESTS

To assess the degradation process, the insulation system is exposed to different thermal stresses that exceed the critical temperature to accelerate the degradation process. Table 1 shows the accepted temperature indices of insulation materials according to IEC 60085. Then, a sufficient amount of degradation data is collected and employed in a reliability assessment procedure. This procedure is so-called accelerated degradation test (ADT) [26]. Through ADTs, the insulation performance is observed as it degrades under elevated thermal stresses. Failure is assumed to occur when the insulation performance degrades below a specified value.

TABLE 1. Thermal classification of rotating machine insulation materials [31].

Letter Classification	Maximum Permissive Temperature (°C)
A	105
E	120
B	130
F	155
H	180

Fig. 1 depicts the non-linear relationship between thermal stress and the measured insulation resistance in an exemplary rectangular copper wire with Class *H* insulation. Additionally, Fig. 1 shows why degradation data, collected under a single thermal stress level, cannot be directly extended to other stress levels using a deterministic physics-based model like the Arrhenius equation. The main reason is to focus only on thermal stress and neglect the influence of other environmental factors like electrical stress, mechanical stress, and ambient conditions that add uncertainty to the degradation process.

Thus, developing an accurate predictive model for insulation degradation should be able to capture the interplay

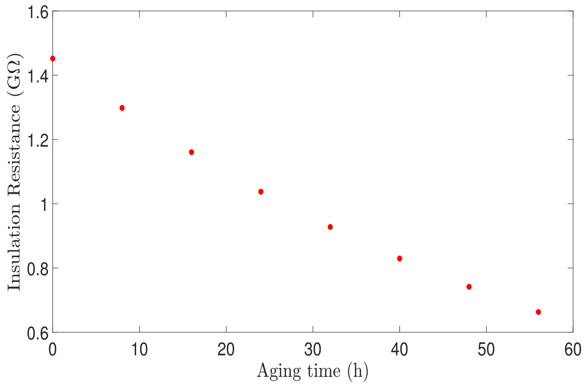

FIGURE 1. Insulation resistance changes with respect to the aging time at 290°C. Adapted from [38].

between deterministic factors, such as the direct and predictable impact of stress level on the degradation rate, and stochastic influences, such as environmental fluctuations.

B. DEGRADATION ESTIMATION USING GAUSSIAN PROCESS REGRESSION

Bayesian inference is widely used as a way of making statistical inferences in which the statistician assigns subjective probabilities, so-called prior distribution, to the distributions that could generate the data [34]. Within the Bayesian regression framework, Gaussian processes (GPs) are popular for constructing "surrogates" of data sources that are difficult to query. GPR is a regression framework to predict a set of function values using GPs, and instead of fitting a single deterministic function to the data, GPR models the relationship between inputs and outputs as a distribution over functions.

An accurate GPR can often be constructed using only a relatively small set of training samples (e.g. tens to hundreds), which consists of pairs of input parameters and corresponding response values. A GP is completely defined by its mean and covariance function. The prediction $f = [f(x_1), f(x_2), \ldots, f(x_N)]^T$ of a GP can be expressed as

$$p\,(f|X) = \mathcal{N}\,(f;\, \mu(X), K(X,X)) \tag{2}$$

where $\mu(X)$ denotes mean function consisting

$$\mu(X) = [\mu(x_1), \mu(x_2), \ldots, \mu(x_N)]^T\,,$$

and $K(X,X)$ is the covariance kernel matrix with entries $\left[K\left(x_i, x_j\right)\right]_{1\le i,j\le N}$ where x_i and x_j are different training samples. The covariance kernel function, $K\left(x_i, x_j\right)$, must be symmetric and positive semi-definite.

The choice of a covariance kernel can have profound impacts on GP predictions. The covariance matrix generated by the kernel function represents the nature of the stochastic process, the uncertainty in the predictions, and cross-correlation between samples. As an example, the squared exponential (SE) kernel defined by

$$K\left(x_i, x_j\right) = \eta^2 exp\left[-\frac{1}{2}\sum_{l=1}^{d}\left(\frac{x_i^l - x_j^l}{\rho_l}\right)^2\right]\eta,$$
$$\rho_1, \ldots, \rho_d \in \mathbb{R} \tag{3}$$

is the most popular kernel assuming that the underlying function is smooth and infinitely differentiable.

In the case of insulation degradation, long-term exposure to elevated temperatures triggers a series of chemical reactions within the insulation material. The rate of oxidation can be roughly described as a first-order chemical reaction with the reaction rate following the Arrhenius rate law, Eq. (1), and the chosen kernel should be able to mimic this exponential decay [35]. In this case, one limitation of the SE kernel is leading to over-smoothing in cases where the degradation path has sharp changes or sudden drops. As a result, a kernel so-called linear ordinary differential equation (LODE) is defined, which incorporates the physical process governing the system and underlies physical reality. Eq. (4) expresses insulation degradation effectively through

$$K\left(x_i, x_j\right) = \sigma^2 exp\left(-0.5(x_i + x_j)/\Theta^2\right) \tag{4}$$

with hyper-parameters σ^2 scaling posterior covariance which can be set to 1 when we are only interested in finding the mean value for the sake of simplicity, and $\Theta = I \cdot \theta$ with $\theta_i > 0$ as the length-scale parameters for each dimension i, and identity matrix I.

To emphasize how the choice of kernel affects the model's behavior, Fig. 2 illustrates different samples of an exemplary random process using different kernels.

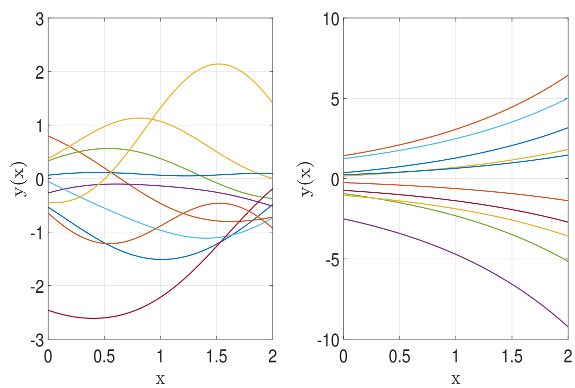

FIGURE 2. The effect of choosing different kernels on the prior function distribution of the Gaussian process. Left is SE kernel (Eq. (3)). Right is LODE (Eq. (4)) in a one-dimensional input space. Each plot includes 10 samples of the random process meaning each line defines one sample of the stochastic process. The distribution of these functions reflects the GP's belief about the underlying process before any data is observed, with variability controlled by the kernel's length-scale parameter.

In Fig. 2, each kernel brings distinct characteristics to the model, impacting how well it captures the underlying dynamics of the process. For example, SE kernel might introduce unnecessary fluctuations or smooth the process in a way that deviates from the actual behavior, while LODE kernel might better reflect the process's true nature, such as capturing an exponential decay. However, Matern kernel is a generalization of the SE kernel, controlled by a smoothness parameter (ν). It can model rougher functions by adjusting ν to model more irregular or sudden changes. But, this smoothness parameter requires careful tuning to match the characteristics of degradation process.

Equation (2), determined by the covariance kernel, K, and the mean function, μ, is referred to as a prior probability density function (PDF) for the GP.

By introducing the actual observation vector, $y = [y(x_1), y(x_2), \ldots, y(x_N)]^T$, disturbed by the Gaussian noise with covariance σ^2, the probability of observing data y, can be expressed as

$$p(y|X, f) = \mathcal{N}\left(y; f, \sigma^2 I_N\right) \sigma \in \mathbb{R} \tag{5}$$

where I_N is the the $N \times N$ identity matrix. The parameters in the covariance kernel function of a GP are referred to as hyper-parameters of the GP, and $\theta_{SE} = [\eta, \rho_1, \ldots, \rho_d, \sigma]$ is defined as the hyper-parameter vector for the squared exponential kernel. In general, finding the best hyper-parameters to fitting the data is an important step of GPR known as training.

MLE offers a solution to find optimized values of the hyper-parameters in terms of the most likely parameters given the observed data. By assuming a GP with a zero-mean prior, the log-likelihood function can be expressed as

$$\begin{aligned}\log p(y|X, f) = &-\frac{1}{2} y^T \left(K(X, X) + \sigma^2 I_N\right)^{-1} y \\ &- \frac{1}{2} \log \left|K(X, X) + \sigma^2 I_N\right| - \frac{N}{2} \log 2\pi.\end{aligned} \tag{6}$$

Then, equation (6) can be optimized to give the most likely values of the hyper-parameters given data.

Once the hyper-parameters of the GPR have been chosen, the posterior of the GP is given by Bayes' rule as

$$p(f|X, y, \theta) = \frac{p(f|X, \theta)\, p(y|X, f, \theta)}{p(y|X, \theta)}. \tag{7}$$

Given (2) and (5), the prediction, $\hat{f}$, of a GPR at a new point, x^*, can be calculated as

$$p\left(\hat{f}|y, X, x^*, \theta\right) = \mathcal{N}\left(\hat{\mu}(x^*), \hat{\nu}(x^*)\right), \tag{8}$$

where

$$\begin{aligned}\hat{\mu}(x^*) &= K(x^*, X)\left(K(X, X) + \sigma^2 I_N\right)^{-1} y, \\ \hat{\nu}(x^*) &= K(x^*, x^*) \\ &\quad - K(x^*, x^*)\left(K(X, X) + \sigma^2 I_N\right)^{-1} \left[K(x^*, X)\right]^T.\end{aligned} \tag{9}$$

It should be noted that $\hat{\mu}(x^*)$ of this Gaussian posterior is the expected value of the predicted function value $\hat{f}$ at x^*, and $\hat{\nu}(x^*)$ is the estimated prediction variance of the same quantity.

III. MODEL CONVERSION FROM ACCELERATED STRESS LEVEL TO WORKING STRESS LEVEL

To achieve a general degradation model by taking the estimated model using GPR and ADT data, an acceleration factor is defined [36]. The relationship between the model parameters and the accelerated stress level is derived by this factor. The acceleration factor can be expressed as

$$A_{12} = \frac{\theta_1}{\theta_2} \tag{10}$$

where θ_1 and θ_2 are hyper-parameters at stress levels 1 and 2 respectively. In the case that temperature stress is the main stress affecting the degradation process, the Arrhenius model is commonly adopted to describe the relationship between temperature stress and the degradation model parameters [26].

According to the estimated degradation path through GPR, higher stress levels result in decreasing the correlation between observations as the time gap between them increases. In other words, the degradation rate of correlation with time increases as the stress level increases. Referring to GPR, the length scale parameter controls how quickly the correlation between observations degrades with time. This causes the length scale parameter to decrease with increasing stress levels.

In other words, the activation energy (E_a) in the Arrhenius equation represents the energy barrier for degradation processes in the insulation material. The temperature dependence of the length-scale parameter reflects how this energy barrier influences the spatial correlations and smoothness of degradation patterns observed over time. Based on these conditions, θ_1 can be defined as:

$$\theta_1 = M \cdot exp\left(\frac{E_a}{kT_1}\right) \tag{11}$$

where T_1 is the temperature accelerated stress level expressed in Kelvin, M is a constant related to the degradation rate in this stress level, E_a and k represent the activation energy and the Boltzmann constant ($k = 8.6171 \times 10^{-5} eV/K$) respectively. Now, the acceleration factor in (10) can be reformulated as

$$A_{12} = \frac{\theta_1}{\theta_2} = exp\left[\frac{E_a}{k}\left(1/T_1 - 1/T_2\right)\right] \tag{12}$$

in which E_a/k needs to be estimated using ADT data sets. Then, hyper-parameters at the normal working stress level, θ_n at T_n, can be derived as

$$\theta_n = \theta_1 \cdot exp\left[\frac{E_a}{k}\left(\frac{1}{T_n} - \frac{1}{T_1}\right)\right] \tag{13}$$

IV. ESTIMATING REMAINING USEFUL LIFE (RUL)

Following the training phase, wherein the GPR model is calibrated using historical data on insulation degradation, predictions are extrapolated into the future to encompass the extended lifetime. The critical task of determining the temporal intersection where degradation surpasses a predefined threshold is accomplished through a systematic iterative procedure.

Specifically, this involved scanning through the predicted degradation trajectory to identify the initial instance where the estimated degradation level exceeds the pre-established threshold. This approach is recognized as the first hitting time (FHT) concept and expressed as

$$LT = inf\,\{t : \mu(t) \geq Threshold\}\,,$$

where *Threshold* denotes the predefined degradation threshold value. Although in GPR the degradation increments are normally distributed, the cumulative process of reaching the *Threshold* leads to an inverse Gaussian distribution as it is influenced by the accumulated uncertainty over time. The probability density function (PDF) of the insulation lifetime can be approximated using the $\hat{\mu}(x^*)$ and $\hat{\nu}(x^*)$ from (9) as

$$f(t|\hat{\mu},\hat{\nu}) = \sqrt{\frac{\lambda}{2\pi t^3}}exp\left(\frac{-\lambda\left(t-\hat{\mu}\right)^2}{2t\hat{\nu}^2}\right), \tag{14}$$

in which, $\lambda = \frac{\mu^3}{\nu^2}$ defines the shape parameter in the inverse Gaussian distribution. However, it's crucial to consider the limitations of extrapolating GPR predictions beyond the training data range. Fig. 3 clearly describe the purpose and the main idea behind the process of estimating insulation degradation using GPR.

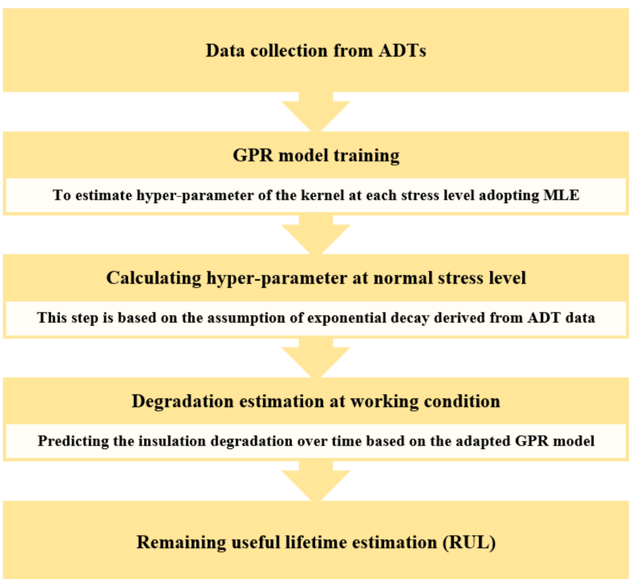

FIGURE 3. Flowchart for estimating insulation degradation and remaining useful lifetime using GPR.

V. SIMULATION RESULTS

Experimental results in different literature illustrate that insulation degradation follows an exponential trend under thermal aging [37], [38]. This fact is the key to choose the kernel function, which mainly defines the local and in some cases global features of the approximated function.

We are grateful to Prof. Kai Wang for generously sharing their dataset on the insulation degradation monitoring [33]. This data was instrumental in allowing us to validate the simulation results through the experimental data. In these ADTs, the outer radius of a magnet wire (see [33] for the insulation information) is measured after each accelerating cycle, and ten cycles of the ADTs are carried out under the accelerated aging temperature of 210°C, 220°C, and 230°C respectively.

To validate the results, the estimated GPR model and its corresponding measured data are drawn under three different thermal stresses in Fig. 4, Fig. 5, and Fig. 6.

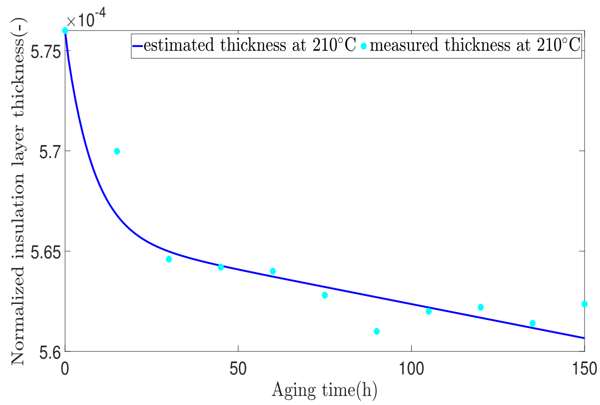

FIGURE 4. Experimental thermal aging data and corresponding GPR approximation at 210°C.

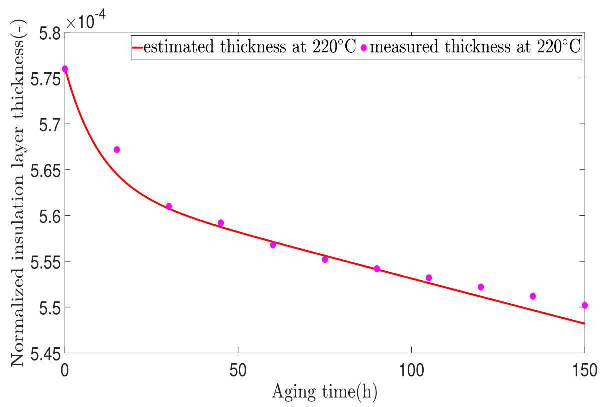

FIGURE 5. Experimental thermal aging data and corresponding GPR approximation at 220°C.

To find the optimal value for kernel hyper-parameter, MLE is employed to find θ in (4) using ADT data, and then (13) is adopted to calculate θ at working condition. Fig. 7 shows the results based on the fact that below a threshold (e.g. 180°C for tested insulation in these experiments), no thermal aging will occur [39].

Physically, the decrease in the length-scale parameter with increasing temperature indicates that the degradation processes in the insulation material become more active or accelerated at higher temperatures. This could be due to various factors, such as increased molecular mobility,

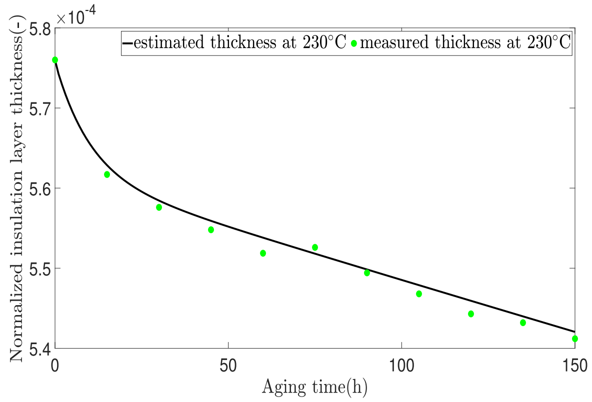

FIGURE 6. Experimental thermal aging data and corresponding GPR approximation at 230°C.

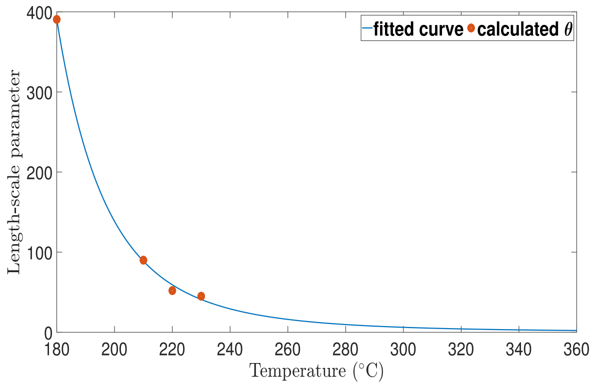

FIGURE 7. LODE hyper-parameter, θ, estimation with respect to different temperature to derive it at working stress level.

enhanced chemical reactions, or higher rates of diffusion of reactive species within the material. To prove this, if a θ is chosen from Fig. 7 at a higher temperature (e.g. 250°C), a more severe degradation is expected during the aging time, and Fig. 8 shows how the insulation thickness changes when it is exposed to 250°C.

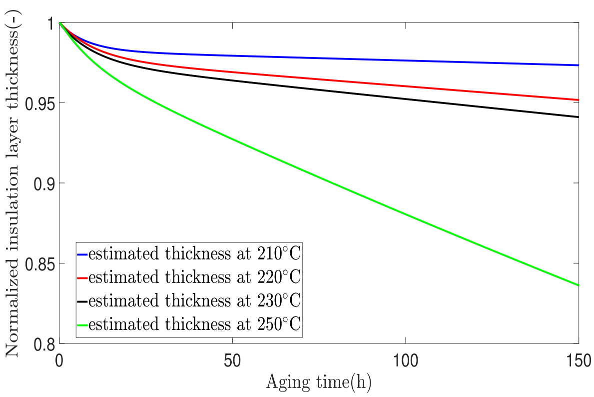

FIGURE 8. Comparing insulation thickness estimation using calculated hyper-parameter at 250°C to other thermal stress levels.

Additionally, to assess the estimation accuracy at each thermal stress, ADT data is divided into training sets to train the GPR model, and validation sets to evaluate how well the model generalizes to new, unseen data. To do so, ADT data for each thermal stress is divided into 80% for training and 20% for validation, ensuring that the model has sufficient data to learn from while providing a robust and representative validation set for performance evaluation. Based on the k-fold cross-validation concept, each data set is divided into 5 subsets, and the model is trained 5 times, each time using 5-1 folds for training and the remaining fold for validation. we can choose any 2 cycles for validation and the remaining 8 cycles for training. There are 45 possible ways to select 2 cycles out of 10 for validation. Each combination gives a different training and validation set. Here, we combine cycles 1 and 2 as the first subset, numbers 3 and 4 as the second subset, numbers 5 and 6 as the third subset, numbers 7 and 8 as the fourth subset, and 9 and 10 as the fifth subset. Then, by defining the relative estimation error (E_r) by

$$E_r = \frac{|deg_{es} - deg_{ex}|}{|deg_{ex}|}, \tag{15}$$

where deg_{es} and deg_{ex} are the GPR estimated mean and measured degradation respectively, the accuracy is evaluated as shown in Fig. 9. Furthermore, Fig. 10 depicts the relative error of degradation estimation, in one of the chosen cases where the fifth subset is chosen for validation. Also, this plot depicts consistent statistical properties in estimation error throughout the different stress levels meaning that the temperature-dependent model to derive hyper-parameter, θ, is sufficient and other factors likely have minimal influence since there's no clear trend in the error signal beyond temperature's effect.

Now, to illustrate the usefulness of the proposed method, the results of adopting GPR in degradation estimation in insulation systems are compared to the Wiener-process-based model since it is commonly used to model degradation processes. Mathematically, a nonlinear Wiener-process degradation model can be described by

$$D(t) = D(0) + \lambda(t) + \sigma_B B(t), \tag{16}$$

where $D(\cdot)$ denotes the degradation path, $D(0)$ is the initial value of the degradation status, $\lambda(t)$ is a nonlinear function providing the drift coefficients representing the average rate of degradation over time, σ_B is the diffusion coefficient representing the volatility or uncertainty in the degradation process, and $B(t)$ is a standard Brownian motion term defining the random fluctuations. This study uses power function $\lambda(t) = \alpha t^{\beta}$, which is widely used when the degradation process exhibits a nonlinear trend over time. Here, MLE is employed to find the optimal values of α, and β.

As can be seen in Fig. 9, when the third subset is chosen for GPR training, the estimation error is higher than other cases (the worst case scenario). Then, Table 2 reports the degradation estimation error at given thermal stresses using GPR (at the worst case scenario according to Eq. (15)), the results of nonlinear Wiener process (NWP) model, and exponential curve fitting (ECF). In case of NWP and ECF, the error is calculated as the difference between the predicted

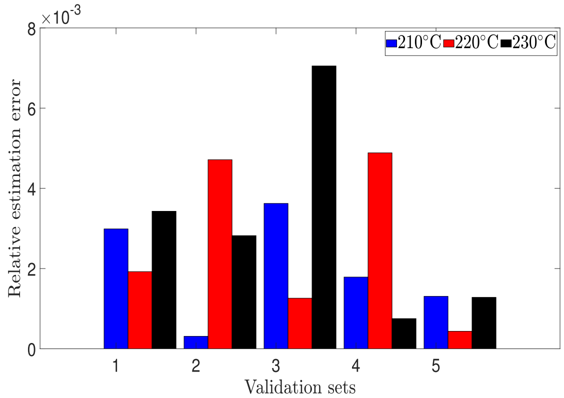

FIGURE 9. Relative error distribution across different validation subsets under 210°C, 220°C, 230°C.

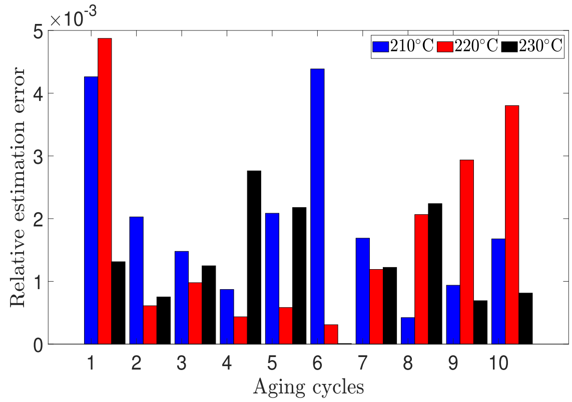

FIGURE 10. Relative error with the last two cycles as validation under 210°C, 220°C, 230°C.

insulation thickness and the observed thickness and then the reported error in Table 2 is the average of all the errors calculated at each sample time within that stress level.

TABLE 2. Degradation estimation errors: GPR vs. Nonlinear wiener Process and exponential curve fitting as a deterministic model.

Thermal stress	GPR error	WP error	ECF error
$210°C$	**0.0038**	0.018	0.0095
$220°C$	**0.005**	0.025	0.0126
$230°C$	**0.007**	0.042	0.019

As demonstrated in the table, GPR consistently results in lower prediction errors compared to ECF and NWP. An important distinction is that GPR provides not only a mean prediction but also confidence intervals, reflecting the uncertainty in the estimated thickness. Table 2, however, focuses on the mean values for simplicity, but the uncertainty provided by GPR gives more information about the reliability of each prediction.

Additionally, the GPR estimation (at the worst case scenario) compared to the results reported in [33] obtained from a commercial solver tool is roughly 71 times more accurate.

As stated in Section IV, the RUL is defined as the hitting time when the insulation thickness crosses a pre-defined threshold as shown in Fig. 11 in which the RUL is defined when estimated degradation path at working condition, e.g. 26°C, exceeds the threshold. Here, 95% confidence interval means that the expected lifetime with 95% likelihood should fall within t_A and t_B and can be modeled using an inverse Gaussian distribution. It is worth mentioning that the decrement in degradation process is not deterministic and the GPR estimated mean values vary, especially in response to external factors such as increasing thermal stress. Then, since the degradation path is probabilistic, the rate of degradation might fluctuate within the uncertainty bounds, even though the mean path might appear smooth.

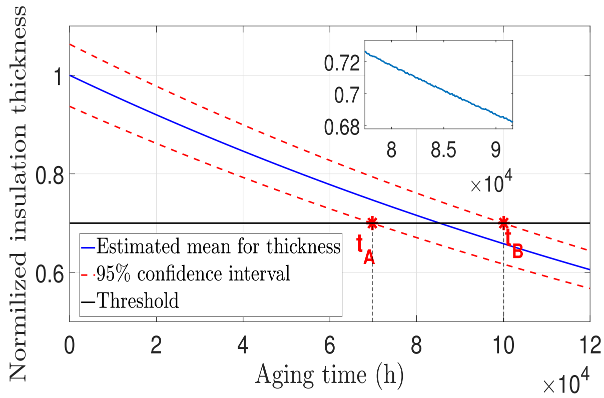

FIGURE 11. Degradation estimation at working stress level with 95% confidence interval.

According to Equation (14), Fig. 12 shows the distribution of estimated lifetime as an inverse Gaussian distribution meaning that the estimated lifetime is distributed within t_a and t_b, with the spread determined by the standard deviation derived from GPR. It dynamically portrays how the estimated RUL evolves over time under working conditions.

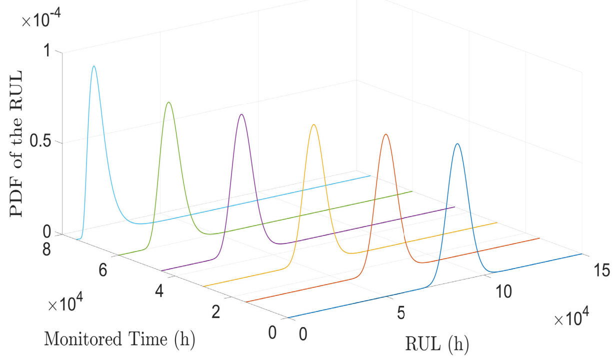

FIGURE 12. The estimated RUL and the corresponding PDF over time for the insulation system.

Fig. 12 displays at lower monitored times, the PDF has a wider range of possible RUL values, indicating greater uncertainty. As the monitored time increases, the distribution narrows which means that the estimated RUL converges towards the mean value and it reflects reduced uncertainty in the RUL estimation.

VI. CONCLUSION

This paper presented a novel approach for estimating the RUL of insulation using GPR and the first-hitting time concept. We employed GPR to model the degradation path of the insulation based on accelerated degradation data under various thermal stresses. The maximum likelihood estimation technique facilitated the identification of optimal hyper-parameters for GPR. Then, incorporating the Arrhenius behavior of the length-scale parameter into the GPR model provided the estimation of hyper-parameters under normal working stress conditions. This approach resulted in the creation of a reliable data-driven RUL model for the insulation.

A significant advantage of this method lies in its utilization of GPR. GPR excels at handling uncertainties inherent in degradation processes without requiring extensive computational effort. Unlike traditional regression techniques that provide only a single point estimate, GPR offers probabilistic predictions. It generates a prediction along with a confidence interval, indicating the range within which the true value is likely to lie. This provides valuable information about the inherent variability and uncertainty associated with the degradation process. GPR's flexibility extends to situations where the noise distribution is unknown which is a common challenge in real-world degradation data with complex noise characteristics.

Our results demonstrate a substantial improvement in estimation accuracy, exceeding previously reported methods by a factor of four at the worst case scenario compared to the Wiener-process-based model. This enhanced accuracy translates to significant benefits for various stakeholders. By enabling more precise predictions of insulation failure, this approach empowers proactive maintenance strategies, minimizing downtime and associated costs. Additionally, it fosters improved safety measures by preventing catastrophic failures.

REFERENCES

[1] P. Zhang, Y. Du, T. G. Habetler, and B. Lu, "A survey of condition monitoring and protection methods for medium-voltage induction motors," *IEEE Trans. Ind. Appl.*, vol. 47, no. 1, pp. 34–46, Jan. 2011.

[2] F. Niu, Y. Wang, S. Huang, L. Wu, X. Huang, Y. Fang, and T. Yang, "An online groundwall insulation monitoring method based on transient characteristics of leakage current for inverter-fed motors," *IEEE Trans. Power Electron.*, vol. 37, no. 8, pp. 9745–9753, Aug. 2022.

[3] J. Cheng, N. Taylor, and P. Werelius, "Nonlinear dielectric properties of the stator and transformer insulation systems," *IEEE Trans. Dielectr. Electr. Insul.*, vol. 29, no. 1, pp. 240–246, Feb. 2022.

[4] P. Giangrande, A. Galassini, S. Papadopoulos, A. Al-Timimy, G. L. Calzo, M. Degano, M. Galea, and C. Gerada, "Considerations on the development of an electric drive for a secondary flight control electromechanical actuator," *IEEE Trans. Ind. Appl.*, vol. 55, no. 4, pp. 3544–3554, Jul. 2019.

[5] M. Popescu, D. A. Staton, A. Boglietti, A. Cavagnino, D. Hawkins, and J. Goss, "Modern heat extraction systems for power traction machines—A review," *IEEE Trans. Ind. Appl.*, vol. 52, no. 3, pp. 2167–2175, May/Jun. 2016.

[6] X. Wang, B. Li, D. Gerada, K. Huang, I. Stone, S. Worrall, and Y. Yan, "A critical review on thermal management technologies for motors in electric cars," *Appl. Thermal Eng.*, vol. 201, Jan. 2022, Art. no. 117758.

[7] V. Madonna, P. Giangrande, L. Lusuardi, A. Cavallini, C. Gerada, and M. Galea, "Thermal overload and insulation aging of short duty cycle, aerospace motors," *IEEE Trans. Ind. Electron.*, vol. 67, no. 4, pp. 2618–2629, Apr. 2020.

[8] W. McDermid and T. Black, "Strategies to maximize life of rotating machines windings," *IEEE Trans. Dielectr. Electr. Insul.*, vol. 22, no. 6, pp. 3087–3098, Dec. 2015.

[9] T. Petri, M. Keller, and N. Parspour, "The insulation resilience of inverter-fed low voltage traction machines: Review, challenges, and opportunities," *IEEE Access*, vol. 10, pp. 104023–104049, 2022.

[10] B. Gorgan, P. V. Notingher, J. M. Wetzer, H. F. A. Verhaart, P. A. A. F. Wouters, A. van Schijndel, and G. Tanasescu, "Calculation of the remaining lifetime of power transformers paper insulation," in *Proc. 13th Int. Conf. Optim. Electr. Electron. Equip. (OPTIM)*, Brasov, Romania, May 2012, pp. 293–300.

[11] G. C. Stone, "Condition monitoring and diagnostics of motor and stator windings—A review," *IEEE Trans. Dielectr. Electr. Insul.*, vol. 20, no. 6, pp. 2073–2080, Dec. 2013.

[12] G. Mazzanti, "Updated review of the life and reliability models for HVDC cables," *IEEE Trans. Dielectr. Electr. Insul.*, vol. 30, no. 4, pp. 1371–1390, Aug. 2023.

[13] M. K. Moghadam, J. Morshedian, M. Ehsani, M. Bahrami, and H. Saddadi, "Lifetime prediction of HV silicone rubber insulators based on mechanical tests after thermal ageing," *IEEE Trans. Dielectr. Electr. Insul.*, vol. 20, no. 3, pp. 711–716, Jun. 2013.

[14] V. Madonna, P. Giangrande, and M. Galea, "Influence of insulation thermal aging on the temperature assessment in electrical machines," *IEEE Trans. Energy Convers.*, vol. 36, no. 1, pp. 456–467, Mar. 2021.

[15] K. Tshiloz, A. C. Smith, A. Mohammed, S. Djurovic, and T. Feehally, "Real-time insulation lifetime monitoring for motor windings," in *Proc. XXII Int. Conf. Electr. Mach. (ICEM)*, Lausanne, Switzerland, Sep. 2016, pp. 2335–2340.

[16] S. R. Rahnamaei, S. M. S. Nejad, A. Rashidi, and A. Sohankar, "Dynamic thermal model for winding temperature of an SRM in an integrated battery charger utilized in electric vehicles," *IEEE Trans. Energy Convers.*, vol. 36, no. 3, pp. 1766–1775, Sep. 2021.

[17] C. Sciascera, M. Galea, P. Giangrande, and C. Gerada, "Lifetime consumption and degradation analysis of the winding insulation of electrical machines," in *Proc. 8th IET Int. Conf. Power Electron., Mach. Drives (PEMD)*, Glasgow, U.K., Apr. 2016, pp. 1–5.

[18] P. Giangrande, V. Madonna, S. Nuzzo, and M. Galea, "Moving toward a reliability-oriented design approach of low-voltage electrical machines by including insulation thermal aging considerations," *IEEE Trans. Transport. Electrific.*, vol. 6, no. 1, pp. 16–27, Mar. 2020.

[19] W. Hassan, F. Mahmood, G. A. Hussain, and S. Amin, "Risk assessment of low voltage motors based on PD measurements and insulation diagnostics," *Measurement*, vol. 176, May 2021, Art. no. 109151.

[20] Y. Zhao, G. Zhang, D. Han, K. Li, Z. Qiu, and F. Yang, "Experimental study on insulation properties of epoxy casting resins using high-frequency square waveforms," *CSEE J. Power Energy Syst.*, vol. 7, no. 6, pp. 1227–1237, Nov. 2021.

[21] M. Dong and A. B. Nassif, "Combining modified Weibull distribution models for power system reliability forecast," *IEEE Trans. Power Syst.*, vol. 34, no. 2, pp. 1610–1619, Mar. 2019.

[22] N. Gebraeel, A. Elwany, and J. Pan, "Residual life predictions in the absence of prior degradation knowledge," *IEEE Trans. Rel.*, vol. 58, no. 1, pp. 106–117, Mar. 2009.

[23] W. Peng, S. P. Zhu, and L. Shen, "The transformed inverse Gaussian process as an age- and state-dependent degradation model," *Appl. Math. Model.*, vol. 75, pp. 837–852, Nov. 2019.

[24] P. Jiang, B. X. Wang, X. Wang, and S. Qin, "Optimal plan for Wiener constant-stress accelerated degradation model," *Appl. Math. Model.*, vol. 84, pp. 191–201, Aug. 2020.

[25] Z. Chen, X. Huang, A. Liu, Y. Ma, J. Zhang, Q. Zhang, R. Wang, and Z. Li, "Reliability-oriented multiobjective optimization of electrical machines considering insulation thermal lifetime prediction," *IEEE Trans. Transport. Electrific.*, vol. 10, no. 1, pp. 2264–2276, Mar. 2024.

[26] Z. Pang, X. Si, C. Hu, D. Du, and H. Pei, "A Bayesian inference for remaining useful life estimation by fusing accelerated degradation data and condition monitoring data," *Rel. Eng. Syst. Saf.*, vol. 208, Apr. 2021, Art. no. 107341.

[27] W. Zhang, B. Li, Y. Lu, J. Li, J. Jiang, and C. Zhang, "Residual lifetime evaluation of power transformer insulation based on PSO-wiener model," in *Proc. IEEE Int. Conf. High Voltage Eng. Appl. (ICHVE)*, Chongqing, China, Sep. 2022, pp. 1–4.

[28] X. Li, Y. Hu, J. Zhou, X. Li, and R. Kang, "Bayesian step stress accelerated degradation testing design: A multi-objective Pareto-optimal approach," *Rel. Eng. Syst. Saf.*, vol. 171, pp. 9–17, Mar. 2018.
[29] H. Deng, W. Hu, D. Cao, W. Chen, Q. Huang, Z. Chen, and F. Blaabjerg, "Degradation trajectories prognosis for PEM fuel cell systems based on Gaussian process regression," *Energy*, vol. 244, Apr. 2022, Art. no. 122569.
[30] W. Hou and Y. Peng, "Adaptive ensemble Gaussian process regression-driven degradation prognosis with applications to bearing degradation," *Rel. Eng. Syst. Saf.*, vol. 239, Nov. 2023, Art. no. 109479.
[31] M. Hashemi, M. Stolz, and D. Watzenig, "Impact of thermal aging on winding insulation loss-of-life fraction using H_∞ algorithm for integrated permanent magnet in-wheel motor," in *Proc. IEEE Int. Automated Vehicle Validation Conf. (IAVVC)*, Austin, TX, USA, Oct. 2023, pp. 1–6.
[32] K. N. Gyftakis, P. A. Panagiotou, N. Lophitis, D. A. Howey, and M. D. McCulloch, "Breakdown resistance analysis of traction motor winding insulation under thermal ageing," in *Proc. IEEE Energy Convers. Congr. Expo. (ECCE)*, Cincinnati, OH, USA, Oct. 2017, pp. 5819–5825.
[33] K. Wang, H. Guo, A. Xu, and M. Pecht, "Degradation monitoring of insulation systems used in low-voltage electromagnetic coils under thermal loading conditions from a creep point of view," *Sensors*, vol. 20, no. 13, p. 3696, Jul. 2020.
[34] C. Jidling, N. Wahlström, A. Wills, and T. B. Schön, "Linearly constrained Gaussian processes," in *Proc. Adv. Neural Inf. Process. Syst.*, vol. 30, 2017, pp. 1215–1224.
[35] C. E. Rasmussen and C. K. I. Williams, *Gaussian Processes for Machine Learning*. Cambridge, MA, USA: MIT Press, 2005.
[36] W. Wei, X. Xu, and Y. Wang, "Remaining life prediction based on Wiener processes with ADT prior information," *Qual. Rel. Eng. Int.*, vol. 32, no. 3, pp. 753–765, 2016.
[37] X. Ge, M. Given, and B. G. Stewart, "A power cable thermal aging insulation resistance degradation model," in *Proc. IEEE Conf. Electr. Insul. Dielectric Phenomena (CEIDP)*, Denver, CO, USA, Oct. 2022, pp. 53–56.
[38] M. R. Khowja, G. Turabee, P. Giangrande, V. Madonna, G. Cosma, G. Vakil, C. Gerada, and M. Galea, "Lifetime estimation of enameled wires under accelerated thermal aging using curve fitting methods," *IEEE Access*, vol. 9, pp. 18993–19003, 2021.
[39] G. Stone, E. A. Boulter, I. Culbert, and H. Dhirani, *Electrical Insulation for Rotating Machines: Design, Evaluation, Aging, Testing, and Repair*, Hoboken, NJ, USA: Wiley, 2004, ch. 2.

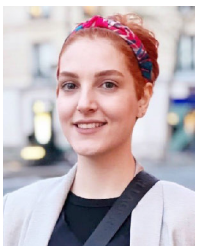

MALIHEH HASHEMI received the M.S. degree in electrical engineering from Iran University of Science and Technology, Tehran, Iran, in 2015. She is currently pursuing the Ph.D. degree in information and communications engineering with Graz University of Technology, Graz, Austria.

She is a Researcher and a Project Assistant with the Institute of Automation and Control, Graz University of Technology. She has authored or co-authored several publications in international conference proceedings. Her current main research interests include electric vehicles, various robust state estimation approaches, health monitoring, and reliability assessment in electric motors.

MICHAEL STOLZ received the M.Sc. degree in mechanical engineering and the Ph.D. degree in control engineering from Graz University of Technology, Graz, Austria.

He is currently a part of the Automated Driving Research Team with the Institute of Automation and Control, Graz University of Technology, as a Postdoctoral Project Assistant. He is also a part of the Control-Systems Group with Virtual Vehicle Research GmbH as a Key Researcher responsible for project management and technical guidance of funded projects in the field of automated driving. He was with the automotive industry as a Development Engineer, for ten years (one year as the Skill Team Leader in the field of automated driving). His main research interests include automated driving, automotive control systems, embedded control, control-system architecture, algorithms for path planning and control, simulation, synchronization, optimization in control, and validation of automated driving.

DANIEL WATZENIG (Senior Member, IEEE) was born in Austria. He received the Ph.D. degree in electrical engineering from Graz University of Technology, Austria.

He is currently the CTO and the Head of the Electronics Systems and Software Department, Virtual Vehicle Research GmbH, Graz. In addition, he was appointed as a Full Professor of multi-sensor perception of autonomous systems with the Institute of Computer Graphics and Vision, Faculty of Computer Science and Biomedical Engineering, Graz University of Technology. He is the author or co-author of more than 200 peer-reviewed articles, book chapters, patents, and articles. His research interests include sense and control of autonomous vehicles, sensor fusion, reinforcement learning, and decision-making under uncertainty.

Prof. Watzenig was awarded the Venia Docendi (Adjunct Professorship) for electrical measurement science and signal processing from Graz University of Technology. Since 2024, he has been the Vice Chair and a member of the Executive Committee of the IEEE Austria Section. He is the Editor-in-Chief of *SAE International Journal on Connected and Automated Vehicles* (SAE JCAV).